

Formation of In nanoparticles on InP wafers by laser-assisted etching

O. R. Musaev · V. Dusevich · J. M. Wrobel ·
M. B. Kruger

Received: 6 September 2010 / Accepted: 16 December 2010 / Published online: 29 December 2010
© Springer Science+Business Media, LLC 2010

Abstract Indium nanoparticles were formed by laser etching an InP (100) wafer in a 10% chlorine–helium atmosphere maintained at $\sim 5\text{--}8 \times 10^{-5}$ Torr. The wafer was irradiated by a homogenized ultraviolet beam with a series of 50–4500 pulses at a fluence of 230 mJ/cm^2 . The surface was also irradiated using fluences from 50 to 340 mJ/cm^2 with 600 pulses. The irradiated surfaces were studied using scanning electron microscopy (SEM), energy dispersive spectroscopy (EDS), and Raman spectroscopy. Raman spectroscopy confirmed that the irradiated surface layer remains crystalline. According to EDS analysis, the surface particles are composed primarily of indium. SEM images show that the number of pulses and the pulse intensity can control the size distribution of the particles.

Introduction

In nanoparticle research, significant effort has been focused on fabricating patterns of nanoparticles on the surfaces of different substrates. One of the approaches to forming nanoparticle arrays on a surface is via self-organization. For example patterns of Fe and Ag, were formed on a Pt surface with a periodic stress-relief pattern [1]. Surface reconstruction of Au has also been used to make self-organized arrays of Co nanoparticles [2]. Vapor deposited In formed Volmer–Weber island arrays on a reconstructed silicon

surface [3]. Beams of Ag nanoparticles have been directed onto a graphite substrate and patterning was achieved via pinning of the deposited clusters to surface defects [4]. The disadvantage of this method is that patterns are periodic and limited by the properties of the materials used.

Lithography is another approach that has been used to fabricate nanoparticle patterns. For example, patterned arrays of Au nanoparticles were assembled by deposition from solution on a lithographically etched resist by means of fluidic effects [5]. Large scale patterning using In nanoparticles on an oxidized Si substrate was achieved by selective charging of the surface, followed by deposition of the In nanoparticles [6]. Since patterning with nanoparticles based on lithography has high costs, alternative approaches have been investigated. For example, near-field optical microscopy was used to develop submicron features [7–9]. The disadvantage of this method is its serial character. A high throughput optical method for patterning of nanoparticles was proposed recently [10]. Here we suggest another, potentially high throughput method for patterning with nanoparticles on a substrate.

Laser-assisted etching in a chlorine atmosphere has been suggested as a possible replacement of more complicated lithographic techniques for patterning of semiconductor surfaces [11–13]. In this work we demonstrate that laser etching can be used for fabrication of In nanoparticles on the surface of a crystal by the preferential removal of P from an InP wafer. This technique could be implemented to produce macroscopic length patterned arrays of nanoparticles with a resolution of $\sim 100 \text{ nm}$.

Experimental

Laser processing of the (100) surface of an InP wafer was performed in a vacuum chamber that could be evacuated to

O. R. Musaev (✉) · J. M. Wrobel · M. B. Kruger
Department of Physics, University of Missouri-Kansas City,
Kansas City, MO 64110, USA
e-mail: musaevo@umkc.edu

V. Dusevich
Department of Oral Biology, University of Missouri-Kansas
City, Kansas City, MO 64110, USA

10^{-8} Torr. After evacuation of air, a 10% chlorine–helium mixture was continuously delivered to the chamber from a gas cylinder through a leak valve, and a pressure of $5\text{--}8 \times 10^{-5}$ Torr was maintained. A pulsed nitrogen laser, Molelectron 1000, with a wavelength of 337 nm, pulse duration of 10 ns and operating frequency of 5 Hz, was used as the light source. The laser beam passed through a multimode optical fiber, and due to redistribution of the energy between transverse electromagnetic modes, became homogenized. A lens produced a 1:1 image of the fiber output on the surface of the wafer inside the chamber.

Indium particles were formed in the illuminated regions on the surface of InP (100) by series of pulses each with a fluence of 230 mJ/cm^2 . The number of pulses were 50, 150, 300, 1500, and 4500. Another four spots containing indium particles were formed by series of 600 pulses and varying fluences: 40, 110, 230, and 340 mJ/cm^2 .

Raman spectra from the processed surfaces were collected using an Acton Research SPI-500 single grating spectrometer equipped with a liquid nitrogen cooled CCD. The 514.5 nm line from an argon-ion laser was used for excitation, with a power of about 12 mW and a diameter of about $40 \mu\text{m}$ at the sample's surface. Scanning electron microscopy (SEM) micrographs were taken with a Philips SEM 515 scanning electron microscope equipped with an energy dispersive spectroscopy (EDS) system. The IMIX-PC, energy dispersive spectrometer was operated at an accelerating voltage of 15 kV and equipped with a Prism detector (Princeton Gamma-Tech, Princeton, NJ).

Results and discussion

For InP etched in a chlorine atmosphere by an excimer laser with a wavelength of 248 nm, it is accepted that Cl_2 molecules spontaneously react with In on the laser heated surface [14, 15]. The indium chloride compounds are volatile and subsequent laser pulses cause thermal desorption of the reaction products [12]. An advantage of this type of etching is that material may be removed at fluences well below the ablation threshold of 140 mJ/cm^2 . For example, etching of InP in a Cl_2 atmosphere has been reported for fluences from 0.15 to 70 mJ/cm^2 [12–15]. The pressure used for etching that provides total removal of indium in the form of volatile reaction products, when using 308 nm radiation and a 10% chlorine–helium atmosphere, is accepted to be 10^{-3} Torr [13].

In the work presented here we irradiated an InP (100) surface by series of pulses with fluences below and above the ablation threshold of InP. However, in order to reduce the rate of the indium–chlorine reaction, we used less than one tenth of the pressure required for total removal of indium ($5\text{--}8 \times 10^{-5}$ Torr). The result of the lowered Cl_2

concentration is that while phosphorus is completely removed, some indium remains on the surface. Since indium does not wet InP, the excess indium coalesces [16]. It forms nanoparticles, which grow due to the release of additional indium atoms from the surface, as well as from the aggregation of neighboring clusters. Indium nanoparticles with sizes from nanometers up to hundreds of nanometers were formed on the surface wherever the laser beam was incident.

Figures 1 and 2 show nanoparticles and histograms of the nanoparticle sizes on the InP wafer that were formed at a fluence of 230 mJ/cm^2 and with 150 and 1500 pulses, respectively. From these figures it is clear that although there remains a large number of small particles there is a difference in the size distribution. The increase in the number of pulses shifted the distribution to larger particle sizes. In Figs. 3 and 4 the images of surfaces irradiated with 600 pulses at fluences of 230 and 40 mJ/cm^2 are shown. From these figures one sees that nanoparticle size is also correlated with increasing laser fluence. Larger particles are formed with increasing fluence. The size dependence of the 100 largest particles on fluence and the number of pulses is shown in Fig. 5. In addition, the particles created with a laser fluence of 40 mJ/cm^2 , tend to be more spherical than those created at 230 mJ/cm^2 . The shape variations can be interpreted as being due to differences in annealing of particles under the low and high fluences. Faceting of the particles formed at higher fluences suggests that they undergo annealing and are crystalline.

A careful examination of Figs. 1, 2, 3, and 4 shows modifications in the surface morphology as well as some correlation between particle location and surface topography. The correlation is strongest in Fig. 3 where valleys and hills are easily observed, as well as the fact that the particles tend to have a higher concentration on the hills than in the valleys. We speculate the particles screen the

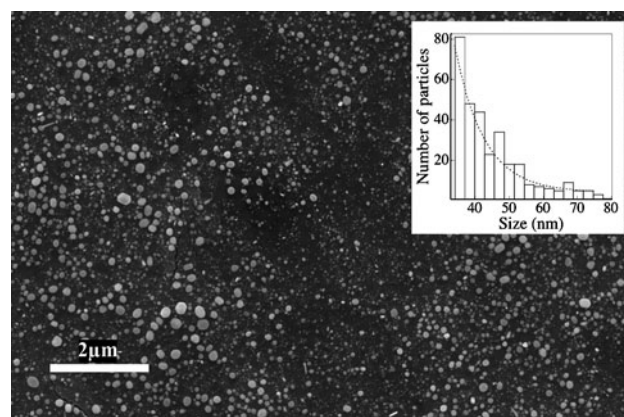


Fig. 1 SEM image and size distribution of particles formed on an InP surface by etching with 150 pulses at a fluence of 230 mJ/cm^2 . Particles smaller than 30 nm were not included in the size distribution

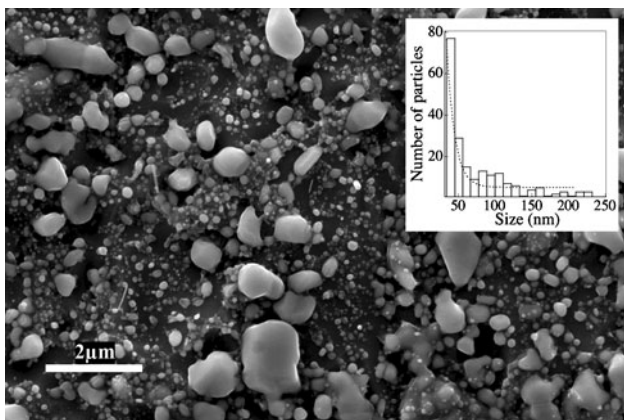


Fig. 2 SEM image and size distribution of particles formed on an InP surface by etching with 1500 pulses at a fluence of 230 mJ/cm^2 . Particles smaller than 30 nm were not included in the size distribution

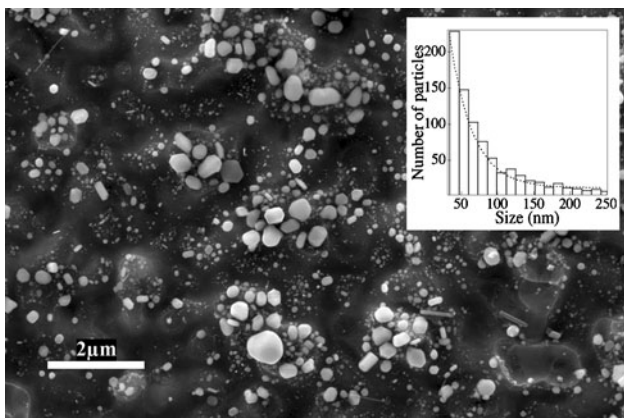


Fig. 3 SEM image and size distribution of particles formed on an InP surface by etching with 600 pulses at a fluence of 230 mJ/cm^2 . Particles smaller than 30 nm were not included in the size distribution

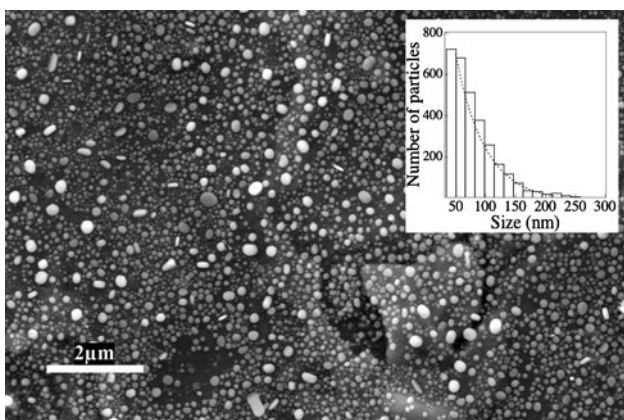


Fig. 4 SEM image and size distribution of particles formed on an InP surface by etching with 600 pulses at a fluence of 40 mJ/cm^2 . Particles smaller than 30 nm were not included in the size distribution

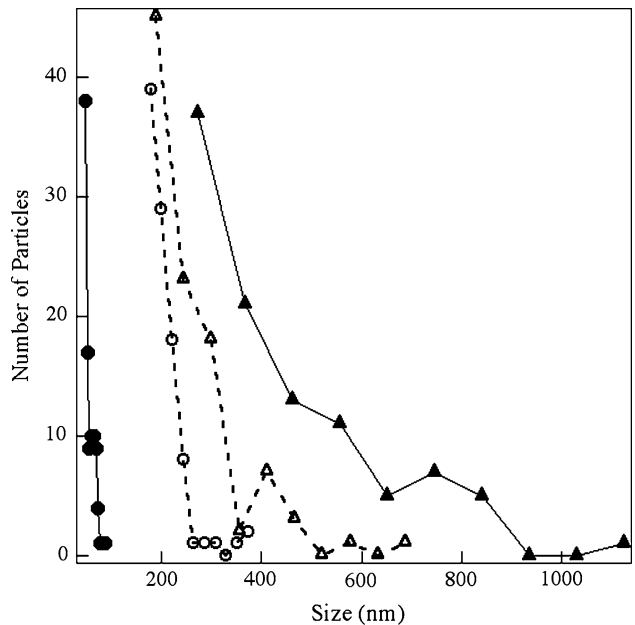


Fig. 5 Particle size distributions for the 100 largest particles created through different etching conditions. *Closed triangles* represent the distribution created with 1500 pulses at a fluence of 230 mJ/cm^2 , *open triangles* represent the distribution created with 600 pulses at a fluence of 230 mJ/cm^2 , *open circles* represent the distribution created with 600 pulses at a fluence of 40 mJ/cm^2 and *closed circles* represent the distribution created with 150 pulses at a fluence of 230 mJ/cm^2

surface from the effects of the laser pulses. Thus, material is preferentially removed from regions that are not covered by particles.

Figure 6a is a SEM micrograph showing two areas from which EDS spectra were collected. The EDS investigations were used to determine the composition of both the particles on the surface (Fig. 6b) and the surface (Fig. 6c), after laser processing with 230 mJ and 1500 pulses. A large particle ($\sim 2 \mu\text{m}$) was chosen for EDS because X-ray photons are collected from a volume with dimensions of up to $1 \mu\text{m}$. Thus the spectrum from region 1 is due only to the particle and there is no contribution from other particles or the surface. The spectrum shows that the particle is composed of almost pure indium. Since phosphorus has a higher vapor pressure than indium, phosphorus is removed preferentially during laser induced heating [17, 18]. Thus, it is reasonable to conclude that the spectrum is representative of all of the surface particles, which are depleted in phosphorus. This seems to be a similar effect to one observed during transmission electron microscopy imaging of InP nanorods. In that work, the electron beam created pure indium nanoparticles on the surface of the InP nanorods [19]. Figure 6c shows an EDS spectrum from the surface, the location identified by spot 2 in Fig. 6a. The

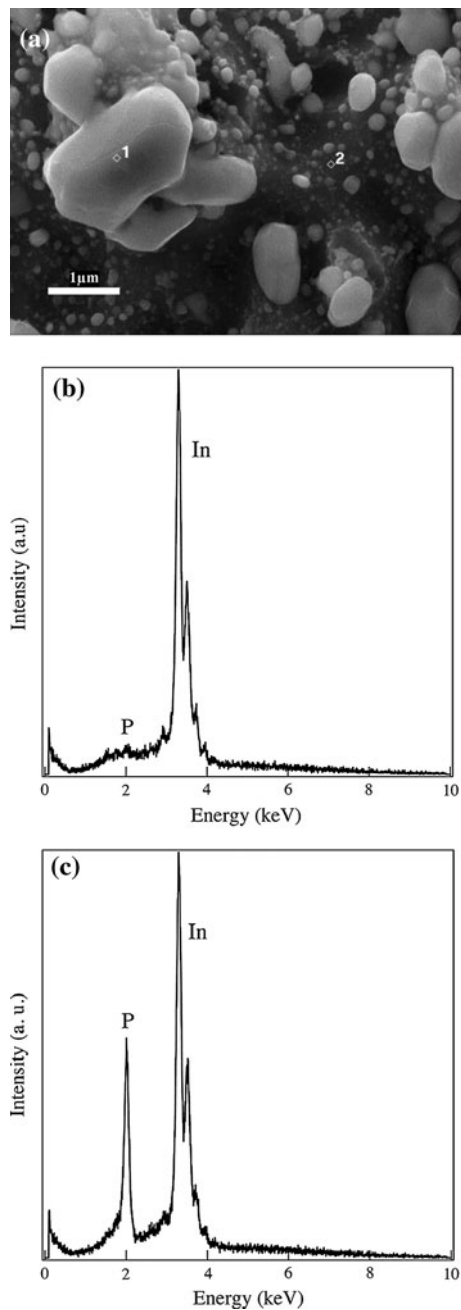


Fig. 6 **a** SEM image of the InP surface after processing with 1500 pulses at a fluence of 230 mJ/cm^2 . **b** EDS spectrum of the particle indicated by position '1' in **a**. **c** EDS spectrum of the surface indicated by position '2' in **a**

spectrum demonstrates that both In and P are present. Due to the particles near spot 2, this spectrum may contain signal from the particles as well as the processed surface. EDS did not detect chlorine on either the surface or the particle.

Background subtracted Raman spectra of the irradiated surface are presented in Fig. 7. From 150 to 1500 pulses there was little change in the spectra. In spite of changes to

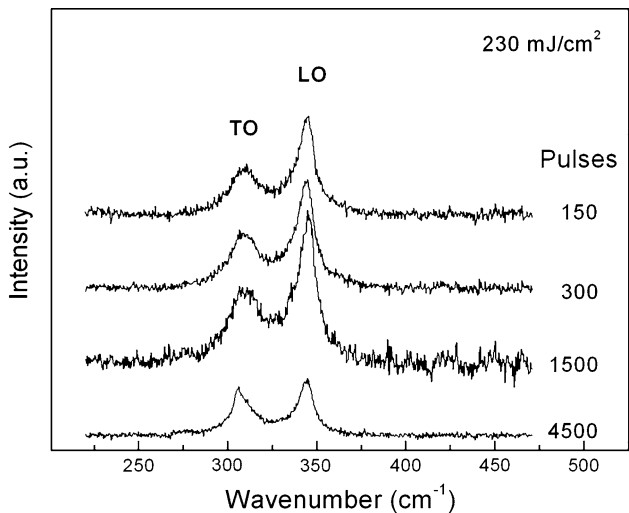


Fig. 7 Raman spectra of InP wafer surfaces after processing at a fluence of 230 mJ/cm^2 and different numbers of pulses

the surface morphology, as seen in the SEM images, the Raman spectra suggest that there was not much damage to the surface crystallinity. However, by 4500 pulses there was a significant change in the longitudinal optical (LO) to transverse optical (TO) intensity ratio. This is most likely due to thermal-plastic deformations. Amplitudes of the LO and TO peaks become equal due to the uniform distribution of (100) as well as (110) facets across the surface [20]. Qualitatively though, the spectra suggest that the surface keeps its crystalline structure [21].

Though formation of nanoparticles of indium in vacuum is possible [16], the presence of chlorine can potentially be used for control of the size distribution. This speculation is based upon the formation of InAs/GaAs quantum dots. In this case the flow of H atoms resulting from decomposition of AsH_3 has a strong effect on the formation regime and properties of quantum dots due to the reactivity of the hydrogen [22–24]. For the current experiment, the presence of chlorine constrains the conditions for forming stable indium clusters, because chlorine reactions with small clusters will eliminate them. The kinetics of cluster growth will depend on the chlorine concentration, which opens the possibility of size distribution control through the partial pressure of chlorine.

Many patterning methods based on self-assembly or direct deposition of clusters, require complex techniques that affect the costs or do not provide the possibility for spatial control of patterning. The present approach offers the possibility to control the size distribution and concentration of particles by using a mask to form an intensity pattern on an InP surface. The light patterning can be made with a resolution of a fraction of a micron and the fabricated patterns can include different sizes of In nanoparticles on the surface of an InP crystal. This approach could

be extended to other III–V (e.g., GaAs) and II–VI semiconductor compounds, for which the vapor pressures of the components are sufficiently different. These materials are popular compound semiconductors and nanopatterning opens possibilities for novel electronic devices.

Conclusion

An alternative method of nanoparticle formation has been demonstrated. A single InP wafer can be used as both the source and substrate for laser-assisted fabrication of In nanoparticles. The size distribution of the indium particles is dependent upon the number of pulses and the fluence. The partial pressure of Cl₂ is one of the factors determining the reaction rate with indium and will also effect the size distribution of the particles. The results suggest that the use of optical masks for laser illumination may allow for the formation of macroscopic scale patterns with features on the order of ~100 nm.

Acknowledgement This work was partially supported by the National Science Foundation Contract numbers, DMR-0605493 and DMR-0923166.

References

1. Brune H, Giovannini M, Bromann K, Kern K (1998) Nature 394:451
2. Chado I, Padovani S, Scheurer F, Bucher JP (2000) Appl Surf Sci 164:42
3. Gruznev DV, Olyanich DA, Avilov VA, Saranin AA, Zotov AV (2006) Surf Sci 600:4986
4. Palmer RE, Pratontep S, Boyen H-G (2003) Nat Mater 2:443
5. Liddle JA, Cui Y, Alivisatos P (2004) J Vac Sci Technol B 22:3409
6. Krinke TJ, Fissan H (2001) Appl Phys Lett 78:3708
7. Chimmalgi A, Grigoropoulos CP, Komvopoulos K (2005) J Appl Phys 97:104319
8. Hwang DJ, Chimmalgi A, Grigoropoulos CP (2006) J Appl Phys 99:044905
9. Sun S, Montague M, Critchley K, Chen M, Dressick WJ, Evans SD, Legett GJ (2006) Nano Lett 6:29
10. Pan H, Hwang DJ, Ko SH, Clem TA, Frechet JMJ, Bauerle D, Grigoropoulos CP (2010) Small 6:1812
11. Heydel R, Maltz R, Göpel W (1995) Appl Surf Sci 69:38
12. Bauerle D (2000) Laser processing and chemistry. Springer, Berlin
13. Wrobel JM, Moffitt CE, Wieliczka DM, Dubowski JJ (1997) SPIE 2991:66
14. Weber H, Matz R, Weimann G (1996) Appl Phys A 63:415
15. Matz R, Weber H, Weimann G (1997) Appl Phys A 65:349
16. Tanaka M, Takeguchi M, Furuya K (1999) Surf Sci 433–435:491
17. Beneking H, Grote N, Selders J (1981) J Cryst Growth 54:59
18. Wada O, Hasewaga H (eds) (1999) InP-based materials and devices: physics and technology. Wiley, New York
19. Golberg D, Mitome M, Yin LW, Bando Y (2005) Chem Phys Lett 416:321
20. Musaev OR, Kwon OS, Wrobel JM, Zhu D-M, Kruger MB (2008) Appl Surf Sci 254:5803
21. Wihl M, Cardona M, Tauc J (1972) J Non-Cryst Sol 8–10:172
22. Heinrichsdorff F, Krost A, Bimberg D, Kosogov AO, Werner P (1998) Appl Surf Sci 123–124:725
23. Li G, Jagadish C (1996) Appl Phys Lett 69:2551
24. Shechukin VA, Bimberg D (1999) Rev Mod Phys 71:1125